Accepted Manuscript

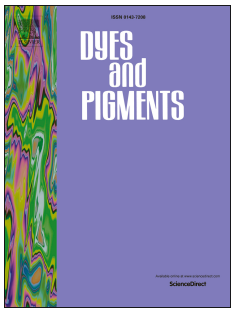

A family of multi-color anthracene carboxyimides: Synthesis, spectroscopic properties, solvatochromic fluorescence and bio-imaging application

Junchao Xu, Guangle Niu, Xiaofang Wei, Minhuan Lan, Lintao Zeng, Joseph M. Kinsella, Ruilong Sheng

PII: S0143-7208(16)31027-0

DOI: 10.1016/j.dyepig.2016.11.056

Reference: DYPI 5625

To appear in: *Dyes and Pigments*

Received Date: 23 October 2016

Revised Date: 30 November 2016

Accepted Date: 30 November 2016

Please cite this article as: Xu J, Niu G, Wei X, Lan M, Zeng L, Kinsella JM, Sheng R, A family of multi-color anthracene carboxyimides: Synthesis, spectroscopic properties, solvatochromic fluorescence and bio-imaging application, *Dyes and Pigments* (2017), doi: 10.1016/j.dyepig.2016.11.056.

Graphical Abstract

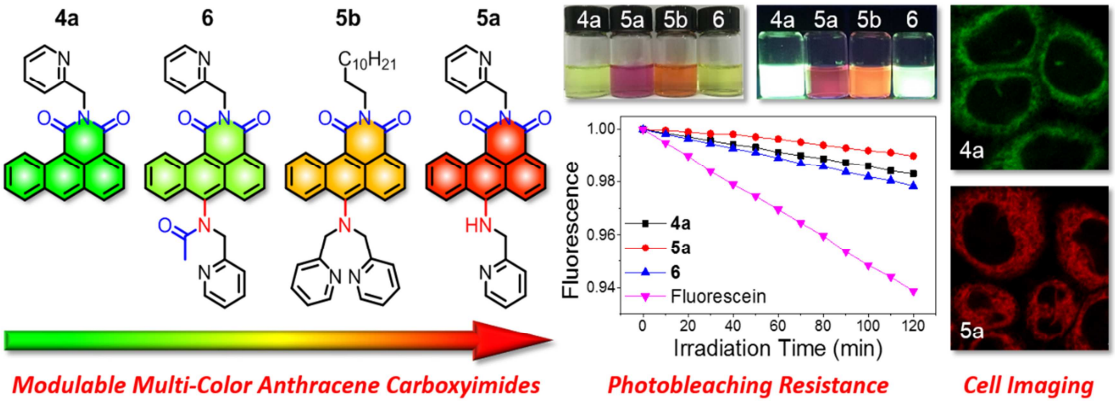

A Family of Multi-Color Anthracene Carboxyimides: Synthesis, Spectroscopic Properties, Solvatochromic Fluorescence and Bio-imaging Application

Junchao Xu[a,#], Guangle Niu[b,#], Xiaofang Wei[b,#], Minhuan Lan[b], Lintao Zeng[a,*], Joseph M. Kinsella[d], Ruilong Sheng[c,d*]

[a] *Tianjin Key Laboratory of Organic Solar Cells and Photochemical Conversion, School of Chemistry and Chemical Engineering, Tianjin University of Technology, Tianjin 300384, P. R. China. E-mail: zlt1981@126.com.* (L. Zeng)

[b] *Key Laboratory of Photochemical Conversion and Optoelectronic Materials, Technical Institute of Physics and Chemistry, Chinese Academy of Sciences, Beijing 100190, P. R. China.*

[c] *Shanghai Institute of Organic Chemistry, Chinese Academy of Sciences, Shanghai 200032, P. R. China. E-mail: rlsheng@mail.sioc.ac.cn.* (R. Sheng)

[d] *Department of Bioengineering, McGill University, 817 Sherbrook Street, Montreal, Quebec, H3A0C3, Canada.*

Abstract:

A family of anthracene carboxyimides with multi-color fluorescence have been successfully prepared, and their spectroscopic properties were investigated by UV-vis absorption spectroscopy, steady-state and time-resolved fluorescence spectroscopy. The photostability and solvatochromic fluorescence in organic solvents were investigated. The parent anthracene carboxyimide **4a** displays very strong green fluorescence (Φ_F = 0.91 in EtOH), good pH stability and photostability, as well as a large Stokes shift. By attachment of different substituents at the 10-position of the anthracene carboxyimide, the fluorescence maxima could be effectively modulated from 500 nm to 615 nm. The 10-(picolylamine) substituted anthracene carboxyimides **5a** and **5b** exhibit large Stokes shifts (> 80 nm) and significant positive solvatochromic fluorescence in organic solvents due to their intramolecular charge-transfer (ICT) character. Furthermore, cell staining experiments indicate that anthracene carboxyimides have excellent cell membrane permeability and good photo-bleaching resistance in living cells. Particularly, compound **5a** is a specific mitochondria-targeting dye with red fluorescence. All these features enable anthracene carboxyimides to serve as promising candidates for bio-labeling/imaging applications.

Keywords: Anthracene carboxyimides, Fluorescence, Solvatochromic, Photostability, Bio-imaging

1. Introduction

Anthracene is a polycyclic aromatic hydrocarbon compound with excellent optical property such as well-resolved absorption and emission band, high fluorescence quantum yield (Φ_F = 0.36 in CH_3CN) and nanosecond lifetime [1, 2]. Anthracene derivatives also exhibit good fluorescence even in the solid state, hence they have been widely used as blue light-emitting materials in organic light-emitting diodes (OLEDs) [3-5]. Despite these advantages, anthracene and its derivatives still cannot meet the criteria for bio-imaging due to some obvious defects including short emission wavelength, poor photostability and water-solubility. For bio-imaging applications, a fluorescent dye with water-solubility, long emission wavelength and large Stokes shift is highly desired, since good water-solubility can enhance the cell/tissue permeability, while long emission wavelength and large Stokes shift can minimize self-absorption and facilitate the penetration of emission light through deep tissues [6-9].

Structurally related to anthracene, perylene and naphthalene are very important members of polycyclic aromatic hydrocarbons, whereas they are hard to be directly used for bio-imaging due to a short emission wavelength (perylene/naphthalene both emit in the deep blue region) [10], poor solubility, and lack of functional groups. For decades, great efforts have been devoted to develop new perylene/naphthalene derivatives with good solubility, long emission wavelength and large Stokes shifts [11]. Among these derivatives, the perylene/naphthalene-based carboxyimides/diimides show fascinating photophysical properties. The fluorescence spectra of perylene/naphthalene carboxyimides are largely red-shifted compared to perylene/naphthalene, and the photophysical properties can be easily modulated by introduction of electron-donating groups on certain position of perylene/naphthalene carboxyimides to form a donor-π-conjugation-acceptor (D-π-A) structure [12-14]. Owing to their good chemical, thermal and photo-stability, the perylene/naphthalene-based carboxyimides/diimides have been successfully applied in the fields of supramolecular assembly [15], organic photovoltaics/transistors [16, 17], bio-labeling [18, 19] and chemosensors [20]. Nevertheless, to our knowledge, anthracene-based carboxyimides/diimides are rarely explored [21-23].

Inspired by the unique properties of perylene/naphthalene-based carboxyimides/diimides, herein, we developed a versatile approach to construct a family of anthracene carboxyimides and modulate

their photophysical properties. In this study, we designed and synthesized a family of anthracene dyes **4a**~**6** (Scheme 1) with the following features: (1) all of these anthracene dyes have a dicarboximide moiety at the 1,9-position to extend the π-conjugation and to serve as strong electron-withdrawing group (EWG), (2) some dyes (**5a**~**5b**) possess substituted amine groups at the 10-position as an electron-donating group (EDG). It is expected that endowing "push-pull" features into the anthracene dyes may result in longer absorption/emission wavelength and large Stokes shifts. The photophysical properties of these dyes were investigated by UV-vis absorption spectroscopy, steady-state and time-resolved fluorescence spectroscopy. Furthermore, cell staining experiments were performed to explore their abilities for bio-imaging application.

2. Results and discussion

2.1 Synthesis

Scheme 1 depicts the synthetic routes and molecular structures of compounds **4**~**6**. Anthracene/ 9-bromoanthracene were used as the starting materials, which reacted with oxalyl chloride *via* Friedel-Crafts acylation to produce the aceanthrylene 1,2-diones (**2a** and **2b**). Subsequently, aceanthrylene 1,2-dione was oxidized by oxone to give the carboxylic acid anhydrides **3a** and **3b** in high yields (~ 90%). Anthracene/9-bromoanthracene have good solubility in organic solvents, while their aceanthrylene 1,2-diones and carboxylic acid anhydrides exhibit poor solubility due to strong π-π stacking and dipole-dipole interactions. Treatment of **3a**/**3b** with an excess of 2-picolylamine afforded the soluble imides **4a**/**5a**. Similarly, treatment of **3b** with 1-aminododecane produced **4b** which exhibited good solubility. These results suggest that introduction of a bulky, sterically demanding group can improve the solubility of these anthracene carboxyimides by disruption of their π-π stacking-induced aggregation [24]. Furthermore, we synthesized compound **5b**, which was incorporated a long alkyl group (1-dodecyl) and a bulky pyridine group to improve the solubility and modulate the spectroscopic properties of anthracene carboxyimides. To further modulate the photophysical property of **5a**, it was reacted with acetyl chloride to afford compound **6** in 65% yield. In this work, pyridine groups were introduced to improve the solubility and modulate the spectroscopic properties for all molecules. As expected, compounds **4a**, **5a**, **5b** and **6** display good solubility in common organic solvents.

2.2 Spectroscopic properties

UV-vis absorption and fluorescence spectra of compounds **4a~6** were measured in EtOH, and the photophysical data were summarized in Table 1. As shown in Fig. 1, compound **4a** displays a characteristic absorption band centered at 436 nm in EtOH, and the maximum emission wavelength is located at 500 nm, which is significantly red-shifted relative to anthracene (λ_{em} = 398 nm in EtOH, Fig. 1). Interestingly, compound **4a** is even more emissive (Φ_F = 0.91 in EtOH) than anthracene (Φ_F = 0.27 in EtOH) [25], which might be attributed to the introduction of the carboxyimide moiety at the 1,9-position of anthracene which inhibits intersystem crossing and photo-induced dimmerization/oxidization [26]. This result suggested that the anthracene carboxyimide moiety not only inherited some good properties of anthracene but also improved its emission efficiency and achieved a remarkable bathochromic (red-shifted) effect on both absorption/emission spectra. Notably, the absorption/emission profiles of **4a** are separated from each other with a relatively large Stokes shift (Fig. 2a), which may be associated with the ICT and asymmetric molecular geometry of **4a** [27]. A large Stokes shift can eliminate the spectral overlap between absorption and emission and allow reliable detection of fluorescence by reducing interference [28]. Moreover, **4a** displays a long fluorescence lifetime (τ_F = 15.18 ns) and a high radiative transition rate constant ($k_r = 0.60 \times 10^8\ s^{-1}$), which enable it to be a good material for bio-imaging.

To further modulate the spectroscopic property of anthracene carboxyimide, we synthesized compounds **5a** and **5b,** which bear electron-donating (amino) groups at the 10-position of anthracene carboxyimides. **5a** exhibits a significant bathochromic shift both in the absorption and emission spectra in comparison with **4a**, whereas the fluorescence quantum yield (Φ_F = 0.07) was dramatically decreased, which was due to the non-radiative decay caused by strong ICT and asymmetric skeleton vibrations in the excited state. By attachment of the di(picolylamine) group at the 10-position of anthracene carboxyimide, **5b** displays moderate fluorescence quantum yield (Φ_F = 0.10) and a large Stokes shift (~109 nm) in EtOH (Fig 2c). The fluorescence spectrum of **5b** was red-shifted by 97 nm in comparison with **4a**, while blue-shifted for 18 nm relative to **5a**. The blue-shift in the UV-vis absorption and fluorescence spectra might be attributed to the electron-withdrawing character of the di(picolyl) group. This result suggests that the spectroscopic properties of anthracene carboxyimides can be effectively modulated by changing the substituent groups at the 10-position. To verify this hypothesis, **5a** was modified with an electron-withdrawing acetyl group at the 10-position to afford compound **6** with an acetylamino structure. As expected, the absorption and fluorescence spectrum

of compound **6** (Fig. 2d) showed dramatic blue-shift ($\lambda_{abs}/\lambda_{em}$ = 437/509 nm) compared to that of **5a** ($\lambda_{abs}/\lambda_{em}$ = 533/615 nm), and the quantum yield (Φ_F = 0.35) was greatly enhanced.

To further understand the fluorescence emission properties of **4a**~**6**, the fluorescence decay traces were fitted by using a monoexponential function (Fig. 3), and the fluorescence lifetimes were determined to be 15.18 (**4a**), 3.56 (**5a**), 5.52 (**5b**) and 1.66 (**6**) ns, respectively. The monoexponential nature of the excited state decays gave evidence for the absence of aggregation of these compounds, which was consistent with the absorption and emission spectra without any sign of aggregates. Importantly, both **5a** and **5b** have shorter excited state lifetimes and lower fluorescence quantum yields than **4a**, which suggests that the non-radiative deactivation of the excited state in **5a** and **5b** were increased by attachment of some electron-donating groups at the 10-position of anthracene carboxyimides. Analogue **6** exhibited very similar absorption/fluorescence feature ($\lambda_{abs}/\lambda_{em}$ = 437/509 nm) to that of **4a** ($\lambda_{abs}/\lambda_{em}$ = 436/500 nm, τ_F = 15.18 ns) but with a shorter fluorescence lifetime (τ_F = 1.7 ns), which elicited that **6** might undergo some non-radiative energy attenuation due to the attached functional groups on the 10-position.

2.3 Solvatochromism fluorescence

To gain an insight into the solvatochromic behavior of these anthracene carboxyimides, the fluorescence and UV-vis absorption spectra were measured in different polarity organic solvents from hexane to EtOH (shown in Fig. 4-5 and Fig. S1-2), and the photophysical properties of anthracene carboxyimides were shown in Table 2. As shown in Fig. 4, the UV-vis absorption spectrum of **4a** is less impressionable to the solvent polarity, whereas the fluorescence spectrum exhibits a significantly positive solvatochromism (red-shift) with increase of the polarity of solvents. This remarkable solvatochromism in fluorescence spectra might be due to an ICT effect. It is well established that ICT compounds usually have large dipole moments in the excited state. Such a polarized excited-state would be stabilized by polar solvents because the dipole-dipole interactions between solvent and ICT compound would reduce the energy of the excited state [29]. For **5a**, significant red-shifts in absorption and emission maxima were observed when the solvent changed from hexane to EtOH. This observation might be due to the strong ICT and intramolecular hydrogen-bond interaction [30] between the -NH- and the pyridyl in **5a**. Likewise, **5b** showed a

pronounced red-shift with the increase of solvent polarity, as shown in Fig. 5. **5a** and **5b** are typical electron donor-π-conjugation-electron acceptor (D-π-A) structured fluorescent dyes with strong ICT characters, which make great contribution to their prominent solvatochromic effects. Owing to the strengthening of dipole-dipole interactions between solute and the solvent, the positive solvatochromism significantly indicated that ICT is involved in all the **4a~6** anthracene carboxyimides.

2.4 Photostability.

Photostability of the fluorescent dye/imaging agent is an important parameter for bio-imaging applications [8]. To investigate the photostabilities of these anthracene carboxyimides, the samples in EtOH were irradiated with a 35 W Xe lamp for 120 min. Fig. 6 shows the photobleaching of **4a**~**6** and the commercially available dye fluorescein, which was monitored by steady-state fluorescence spectroscopy. As shown in Fig. 6, compounds **4a~6** lose less than 2.2% of their fluorescence intensity under the irradiation from a 35 W Xe lamp for 120 min, while the commercial fluorescein loses 6.1%. It is likely that introduction of electron-withdrawing carboxyimide moiety at 1,9-position of anthracene would decrease the HOMO and LUMO energy level, thus inhibits its photo-induced dimmerization/oxidization (photodimerized under UV irradiation) [31]. The good photostabilities of **4a**~**6** make feasible their use as long-term bio-imaging agents for *in situ* visualizing biological events in living cells.

2.5 pH stability

The pH stabilities of these anthracene carboxyimides were evaluated in various pH buffer solutions (50 mM, pH 3~10.5) containing 10% EtOH. As shown in Fig. 7, the fluorescence intensity of **5a** and **6** almost remain stable over a wide range of pH values (3.0~9.0), which were attributed to the insensitive protonation/de-protonation features of aromatic-ring attached amino groups. The anthracene carboxyimides with good pH stability features are favorable for intracellular analysis and imaging because they are less impressionable to the pH inside various subcellular organelles.

2.6. Cell imaging

The excellent fluorescence properties of these anthracene carboxyimides prompted us to test their

ability for bio-imaging in living cells. Cell cytotoxicity of anthracene carboxyimide dyes were examined by Cell Counting Kit-8 (CCK-8), and the results indicated that these dyes have very low cytotoxicity (Fig. S3). HeLa cells were incubated with dye **4a** (10 μM) and a nucleus-specific staining probe Hoechst (1 μM) for 30 min, and then washed with PBS for three times to remove the excessive dye. As shown in Fig. 8c, the nuclei with strong blue fluorescence were observed after incubation with Hoechst. At the surrounding area of nuclei, a clear cell profile with green fluorescence was clearly observed after incubation with **4a**, suggesting that **4a** has permeated into the HeLa cells in a short period. The good cell membrane permeability and fluorescence property of **4a** enable it to be used as a dye/staining agent for bio-imaging in living cells.

As mentioned before, dye **4a** showed good photostability under the irradiation from a Xe lamp. Herein, we also evaluated the long-term imaging capability of **4a** by measuring its photobleaching resistance capability in HeLa cells. As shown in Fig. 9, a clear HeLa cell profile with green fluorescence was observed after incubation with **4a** (10 μM) for 30 min, then the cells were steadily irradiated using a 200 W laser (at 488 nm) for 5 min and the cell images were taken by fluorescence microscope. It could be observed that the fluorescence intensity of HeLa cells was not obviously changed after exposure to UV irradiation for 5 min. The photobleaching resistance feature made **4a** attractive for long-term bio-imaging applications.

The bio-imaging ability of dye **5a** was also examined. HeLa cells were co-incubated with **5a** (10 μM) and Hoechst (1 μM) for 30 min. As shown in Fig. 8g, nuclei with strong blue fluorescence were observed, and a clear cell profile with red fluorescence was observed at the surrounding area of nucleic. To determine the subcellular localization of **5a**, a commercially available mitochondrial dye (MitoTracker Green FM) was used for a co-localization study. HeLa cells were co-incubated with **5a** (10 μM) and MitoTracker Green FM (200 nM) at 37 °C for 30 min. Fig. 10d shows the bright field image of HeLa cells with good cell morphology after incubation with **5a** and MitoTracker Green FM. As shown in Fig. 10b, the cells exhibited a clear mitochondria profile with strong green fluorescence after incubation with MitoTracker Green FM for 30 min. A similar mitochondria profile with red fluorescence was observed from the red channel after incubation with **5a** for 30 min (Fig. 10a). The red fluorescence signal originated from **5a** overlaid very well with the green fluorescence of MitoTracker Green FM (Fig. 10c and f). In addition, Pearson's co-localization coefficient, that describes the correlation of the intensity distribution between two channels, was calculated to be 0.96

(Fig. 10e), confirming that **5a** was site-specifically stained in mitochondria of living cells. This observation might be due to protonation of pyridyl (p*K*b for pyridine is ~8.8) inside the cancer cells, which facilitates it to accumulate in the mitochondria of living cells. The detailed mechanism of the mitochondria localization effect of **5a** is under investigation.

3. Conclusions

In summary, a family of anthracene carboxyimides has been successfully prepared from anthracene/9-bromoanthracene. Their fluorescence maxima could be effectively modulated from 500 nm to 615 nm by attaching various substituent groups to the 10-position of anthracene carboxyimides. These compounds display moderate to high fluorescence quantum yields, good pH stability as well as large Stokes shifts. Additionally, these compounds offer positive solvatochromic fluorescence and good photo-bleaching resistance capability in organic solvents. Cell staining experiments indicate that anthracene carboxyimides have excellent cell membrane permeability and good photo-bleaching resistance in living cells. Particularly, compound **5a** is a specific mitochondria-targeting dye with red fluorescence, which enables it to be a potential mitochondria-staining agent. This research not only developed a versatile approach to construct a family of anthracene carboxyimides with multi-color fluorescence, but also opened an avenue to utilize them for bio-imaging.

Acknowledgments

We gratefully acknowledge the financial support from National Science Foundation of China (No. 21203138, 21372251) and the Opening funding from Key Laboratory of Photochemical Conversion and Optoelectronic Materials, TIPC, Chinese Academy of Sciences. Dr. Ruilong Sheng also appreciates the Chinese Academy of Sciences (CAS) for the CAS-Canada Young Visiting Scientist Scholarship and Youth Innovation Promotion Association (YIPA, No2012204) Scholarship.

References

[1] Pownall HJ, Smith LC. Fluorescence quenching of anthracene in charged micelles by pyridinium and iodide ions. Biochemistry 1974;13:2594-7.

[2] Sugino M, Araki Y, Hatanaka K, Hisaki I, Miyata M, Tohnai N. Elucidation of anthracene

arrangement for excimer emission at ambient conditions. Cryst Growth Des 2013;13:4986-92.

[3] Na EJ, Lee KH, Kim BY, Lee SJ, Kim YK, Yoon SS. Non-doped blue OLEDs based on 9,9′-dimethylfluorene containing 10-naphthylanthracene derivatives. Mol Cryst Liq Cryst 2013;584:113-22.

[4] Lee KH, Kim SO, You JN, Kang S, Lee JY, Yook KS, et al. *tert*-Butylated spirofluorene derivatives with arylamine groups for highly efficient blue organic light emitting diodes. J Mater Chem 2012;22:5145-54.

[5] Seo BM, Seo JH, Kim JH, Park JS, Lee KH, Park MH, et al. Efficient orange-red organic light-emitting diodes using 9,10-bis[4-(di-4-*tert*-butylphenylamino)styryl] anthracene as a fluorescent orange-red emitter. Thin Solid Films 2010;518:6214-8.

[6] Ntziachristos V, Tung CH, Bremer C, Weissleder R. Fluorescence molecular tomography resolves protease activity *in vivo*. Nat Med 2002;8:757-61.

[7] Yuan L, Lin W, Zheng K, He L, Huang W. Far-red to near infrared analyte-responsive fluorescent probes based on organic fluorophore platforms for fluorescence imaging. Chem Soc Rev 2013;42:622-61.

[8] Zeng L, Jiao C, Huang X, Huang K-W, Chin W-S, Wu J. Anthracene-fused BODIPYs as near-infrared dyes with high photostability. Org Lett 2011;13:6026-9.

[9] Xu J, Pan J, Zhang Y, Liu J, Zeng L, Liu X. Ultrasensitive near-infrared fluorescence-enhanced probe for discriminative detection of GSH and Cys from different emission channels. Sens Actuators B 2016;238:58-65.

[10] Motyka AL, Wittmeyer SA, Babbitt RJ, Topp MR. Weak vibrational coupling in a large van der Waals complex: Fluorescence spectroscopy of perylene/naphthalene. J Chem Phys 1988;89:4586-99.

[11] Singh TB, Erten S, Günes S, Zafer C, Turkmen G, Kuban B, et al. Soluble derivatives of perylene and naphthalene diimide for n-channel organic field-effect transistors. Org Electron 2006;7:480-9.

[12] Oh SH, Kim BG, Yun SJ, Maheswara M, Kim K, Do JY. The synthesis of symmetric and asymmetric perylene derivatives and their optical properties. Dyes Pigments 2010;85:37-42.

[13] Sun Z, Ye Q, Chi C, Wu J. Low band gap polycyclic hydrocarbons: from closed-shell near infrared dyes and semiconductors to open-shell radicals. Chem Soc Rev 2012;41:7857-89.

[14] Liu X, Qiao Q, Tian W, Liu W, Chen J, Lang MJ, et al. Aziridinyl fluorophores demonstrate

bright fluorescence and superior photostability by effectively inhibiting twisted intramolecular charge transfer. J Am Chem Soc 2016;138:6960-3.

[15] Addicott C, Oesterling I, Yamamoto T, Müllen K, Stang PJ. Synthesis of a bis(pyridyl)-substituted perylene diimide ligand and incorporation into a supramolecular rhomboid and rectangle *via* coordination driven self-assembly. J Org Chem 2005;70:797-801.

[16] Huang C, Barlow S, Marder SR. Perylene-3,4,9,10-tetracarboxylic acid diimides: synthesis, physical properties, and use in organic electronics. J Org Chem 2011;76:2386-407.

[17] Würthner F, Stolte M. Naphthalene and perylene diimides for organic transistors. Chem Commun 2011;47:5109-15.

[18] Michelia E, D'Ambrosiob D, Franceschina M, Savino M. Water soluble cationic perylene derivatives as possible telomerase inhibitors: the search for selective G-quadruplex targeting. Mini Rev Med Chem 2009;9:1622-32.

[19] Di Antonio M, Doria F, Richter SN, Bertipaglia C, Mella M, Sissi C, et al. Quinone methides tethered to naphthalene diimides as selective G-quadruplex alkylating agents. J Am Chem Soc 2009;131:13132-41.

[20] Erdemir S, Kocyigit O, Karakurt S. A new perylene bisimide-armed calix[4]-aza-crown as "turn on" fluorescent sensor for Hg^{2+} ion and its application to living cells. Sens Actuators B 2015;220:381-8.

[21] Langhals H, Schönmann G, Polborn K. Anthracene carboxyimides and their dimers. Chem Eur J 2008;14:5290-303.

[22] Yao JH, Chi C, Wu J, Loh K-P. Bisanthracene bis(dicarboxylic imide)s as soluble and stable NIR dyes. Chem Eur J 2009;15:9299-302.

[23] Ikbal M, Banerjee R, Atta S, Dhara D, Anoop A, Singh NDP. Synthesis, photophysical and photochemical properties of photoacid generators based on *N*-hydroxyanthracene-1,9-dicarboxyimide and their application toward modification of silicon surfaces. J Org Chem 2012;77:10557-67.

[24] Gao D, Tian K, Zhang W, Huang J, Chen Z, Mao Z, et al. Approaching high charge carrier mobility by alkylating both donor and acceptor units at the optimized position in conjugated polymers. Polym Chem 2016;7:4046-53.

[25] Park CS, Lee JY, Kang E-J, Lee J-E, Lee SS. A highly selective fluorescent chemosensor for

silver(I) in water/ethanol mixture. Tetrahedron Lett 2009;50:671-5.

[26] Grimme S, Diedrich C, Korth M. The importance of inter- and intramolecular van der Waals interactions in organic reactions: the dimerization of anthracene revisited. Angew Chem Int Ed 2006;45:625-9.

[27] Chen Y, Zhao J, Guo H, Xie L. Geometry relaxation-induced large Stokes shift in red-emitting borondipyrromethenes (BODIPY) and applications in fluorescent thiol probes. J Org Chem 2012;77:2192-206.

[28] Qu X, Liu Q, Ji X, Chen H, Zhou Z, Shen Z. Enhancing the Stokes' shift of BODIPY dyes *via* through-bond energy transfer and its application for Fe^{3+}-detection in live cell imaging. Chem Commun 2012;48:4600-2.

[29] Sissa C, Parthasarathy V, Drouin-Kucma D, Werts MHV, Blanchard-Desce M, Terenziani F. The effectiveness of essential-state models in the description of optical properties of branched push-pull chromophores. Phys Chem Chem Phys 2010;12:11715-27.

[30] Reichardt C. Polarity of ionic liquids determined empirically by means of solvatochromic pyridinium *N*-phenolate betaine dyes. Green Chem 2005;7:339-51.

[31] Breton GW, Vang X. Photodimerization of anthracene. J Chem Educ 1998;75:81.

Table 1 Photophysical properties of anthracene carboxyimides **4~6** in EtOH.

Compound	λ_{abs} (nm)	ε ($M^{-1}\cdot cm^{-1}$)	λ_{em} (nm)	Φ_F	$\Delta\nu$ (cm^{-1})	τ_F (ns)	k_r (s^{-1})	k_{nr} (s^{-1})
4a	436	9.60×10^3	500	0.91	2936	15.18	5.99×10^7	5.93×10^6
4b	438	9.87×10^3	505	0.88	3029	—	—	—
5a	533	1.02×10^4	615	0.07	2502	3.56	1.97×10^7	2.61×10^8
5b	488	9.61×10^3	597	0.10	3741	5.52	1.81×10^7	1.63×10^8
6	437	1.08×10^4	509	0.35	3237	1.66	2.11×10^8	3.92×10^8

Table 2 Photophysical properties of anthracene carboxyimides **4a~6** in different solvents.

Compound	Solvent	λ_{abs} (nm)	ε ($M^{-1}\cdot cm^{-1}$)	λ_{em} (nm)	Φ_F	$\Delta\nu$ (cm^{-1})
4a	Hexane	427	1.21×10^4	465	0.61	1914
	Toluene	435	9.50×10^3	483	0.69	2285
	DCM	437	1.01×10^4	490	0.93	2475
	THF	432	9.50×10^3	485	0.83	2530
	EtOH	436	9.60×10^3	500	0.91	2936
5a	Hexane	497	9.87×10^3	594	0.04	3286
	Toluene	517	1.18×10^4	606	0.08	2841
	DCM	527	1.44×10^4	611	0.10	2609
	THF	520	9.10×10^3	609	0.07	2810
	EtOH	533	1.02×10^4	615	0.07	2502
5b	Hexane	480	9.35×10^3	555	0.06	2815
	Toluene	492	8.42×10^3	573	0.06	2873
	DCM	500	9.22×10^3	587	0.12	2964
	THF	497	8.12×10^3	583	0.07	2968
	EtOH	488	9.61×10^3	597	0.10	3741
6	Hexane	432	1.07×10^4	486	0.59	2572
	Toluene	437	1.15×10^4	491	0.52	2517
	DCM	439	1.11×10^4	497	0.48	2658
	THF	436	1.19×10^4	497	0.36	2815
	EtOH	437	1.08×10^4	509	0.35	3237

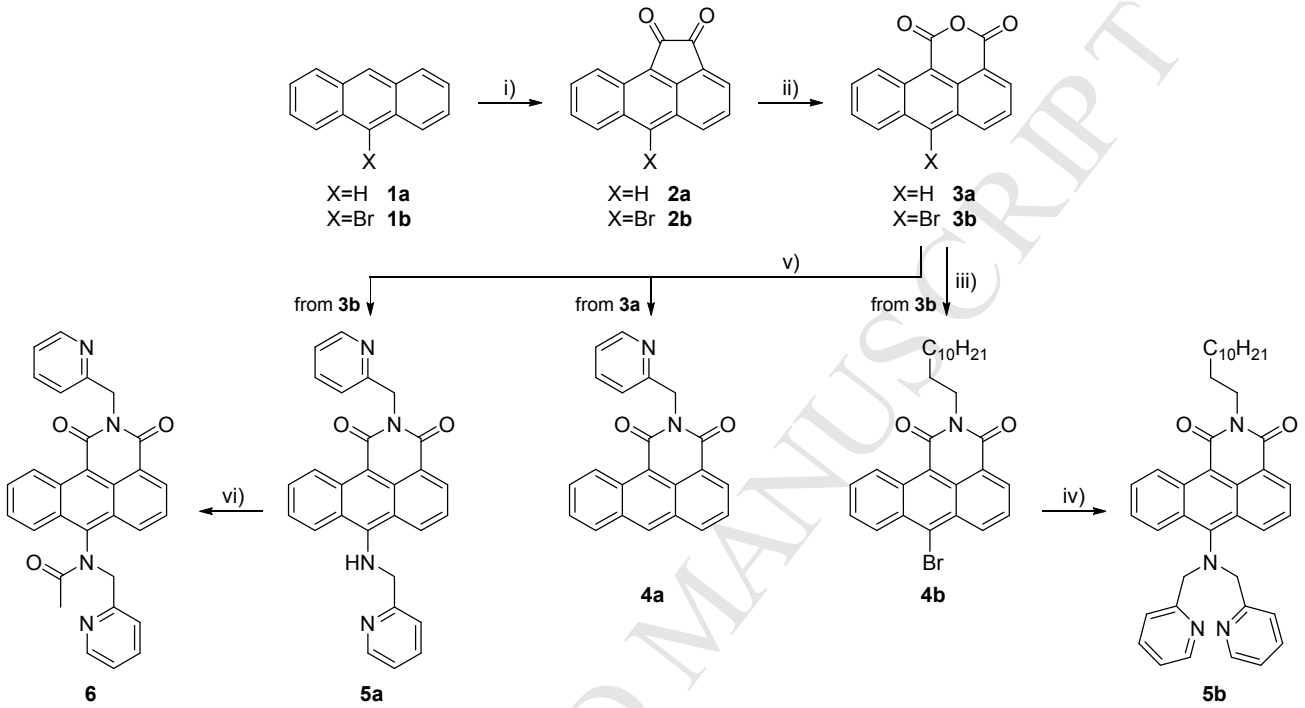

Scheme 1 Synthetic routes for anthracene carboxyimides. i) oxalyl chloride, $AlCl_3$; ii) oxone; iii) 1-aminododecan; iv) 2,2'-dipicolylamine; v) 2-picolylamine; vi) acetyl chloride, K_2CO_3.

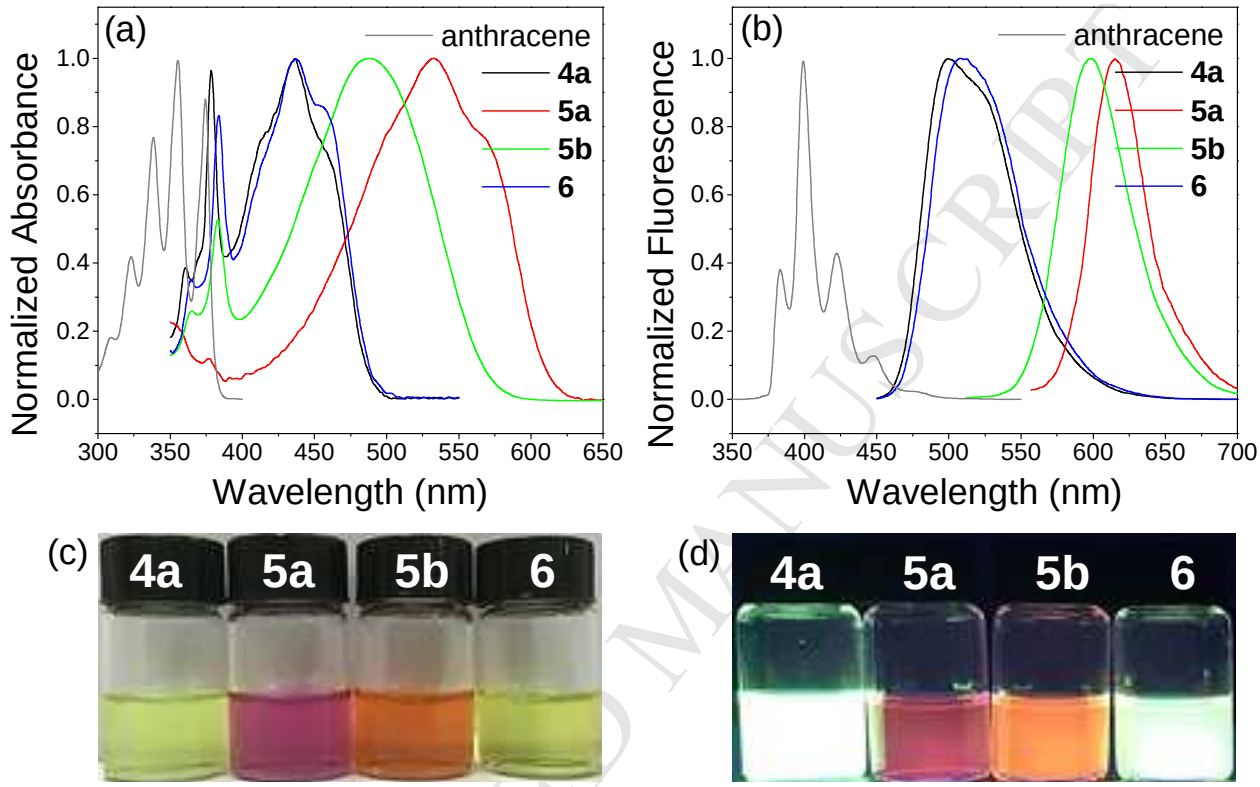

Fig. 1 Normalized UV-vis absorption (a) and fluorescence (b) spectra of anthracene and anthracene carboxyimide dyes in EtOH. Photographs of anthracene carboxyimide dyes under daylight (c) and 365 nm UV lamp (d).

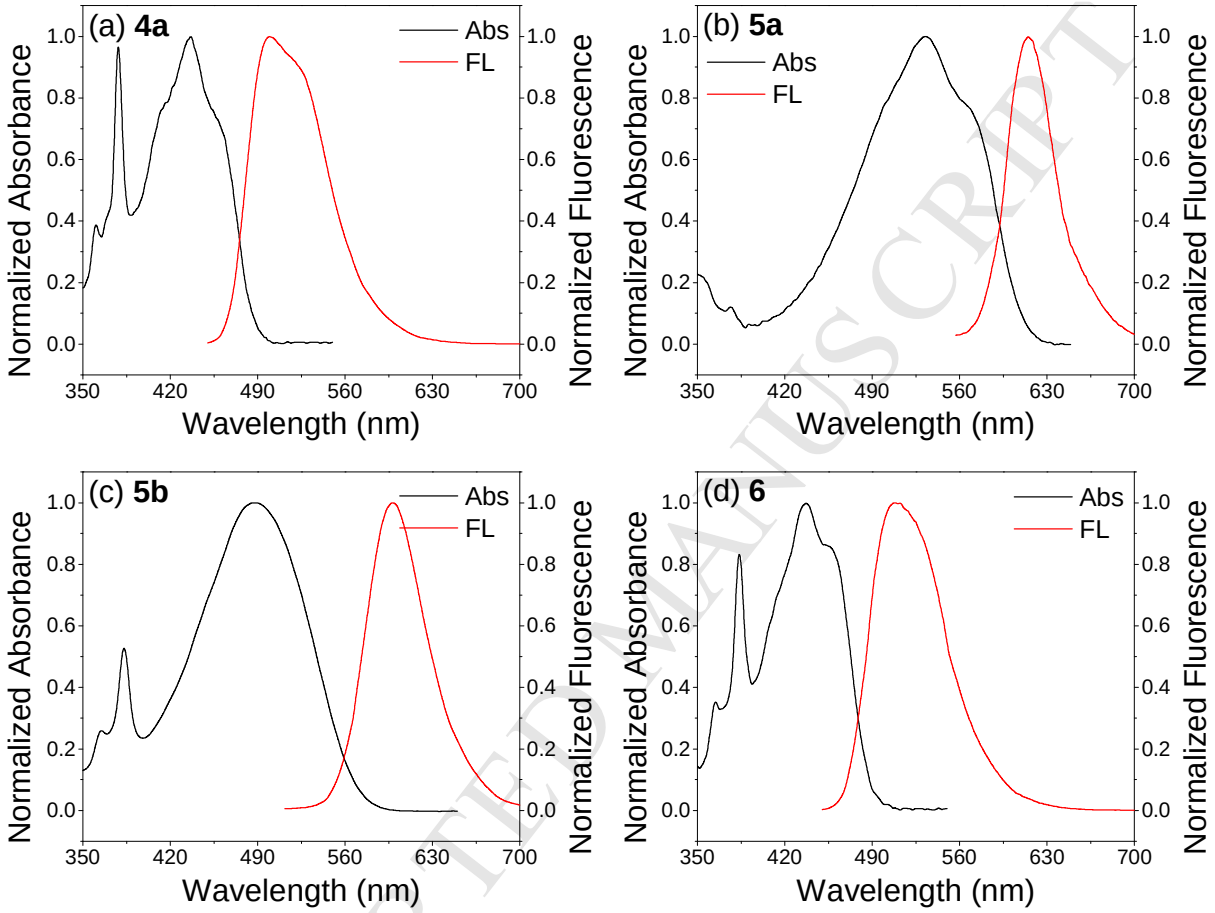

Fig. 2 Normalized UV-vis absorption and fluorescence spectra of **4a** (a), **5a** (b), **5b** (c) and **6** (d) in EtOH.

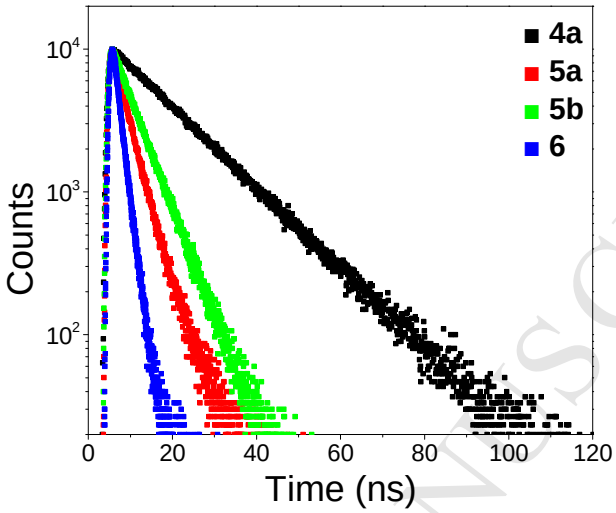

Fig. 3 Time-resolved fluorescence decay traces recorded for **4a**~**6** in EtOH at 25 °C. Excitation wavelength: 480 nm.

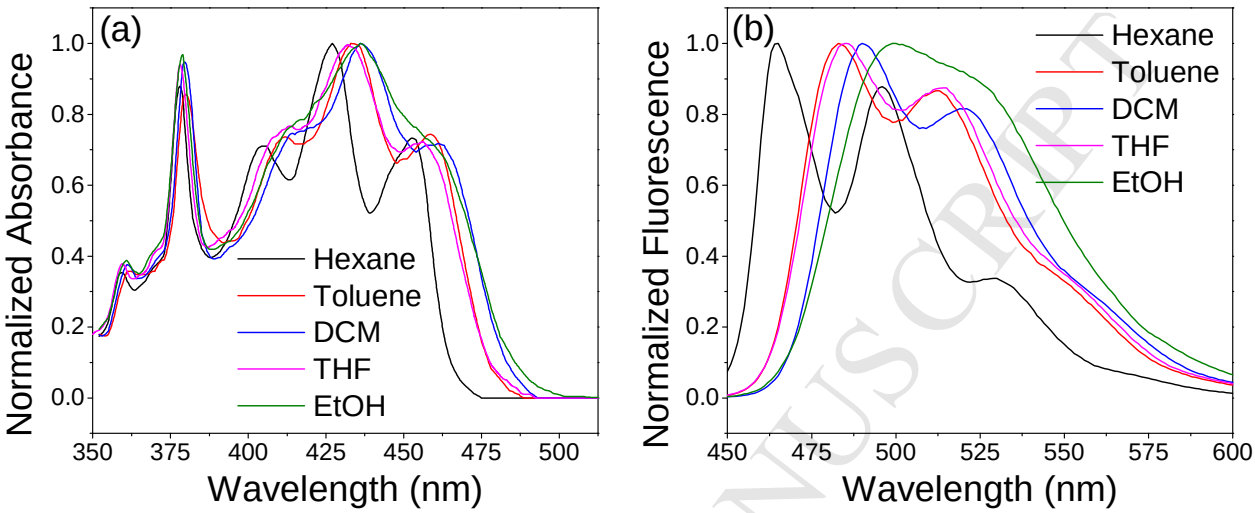

Fig. 4 Normalized UV-vis (a) and fluorescence (b) spectra of **4a** in different solvents.

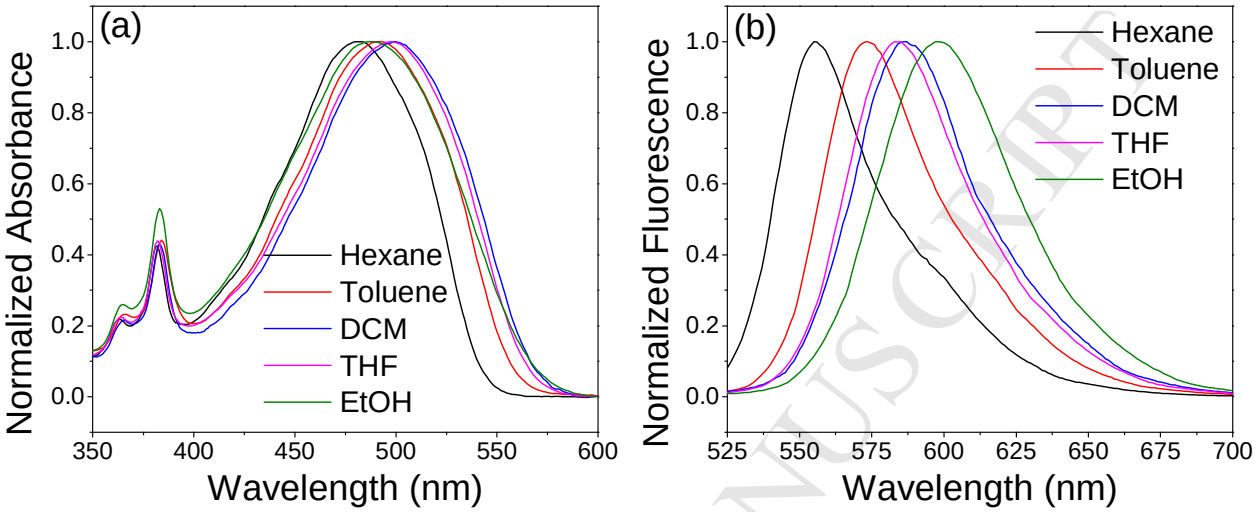

Fig. 5 Normalized UV-vis (a) and fluorescence (b) spectra of **5b** in different solvents.

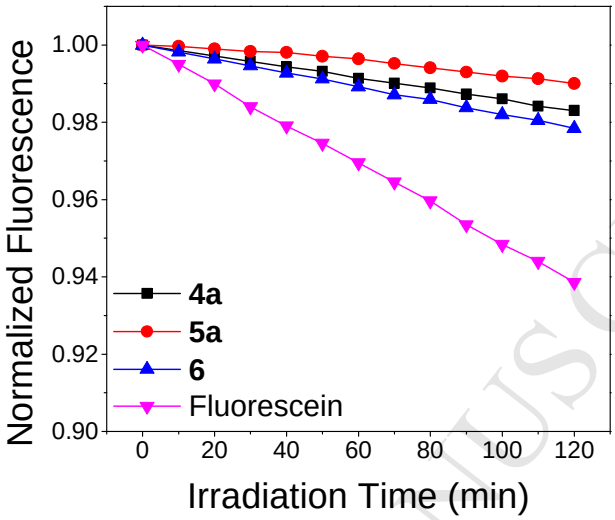

Fig. 6 Changes of fluorescence intensity (c = 10 μM) under the continuous irradiation from a 35 W Xe lamp.

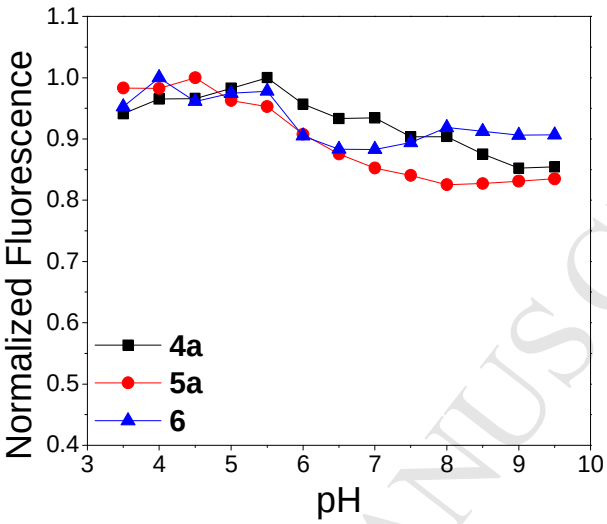

Fig. 7 Changes of fluorescence intensity (c = 10 μM) at different pH values in buffer solution (50 mM, pH 3~10.5, with 10% EtOH).

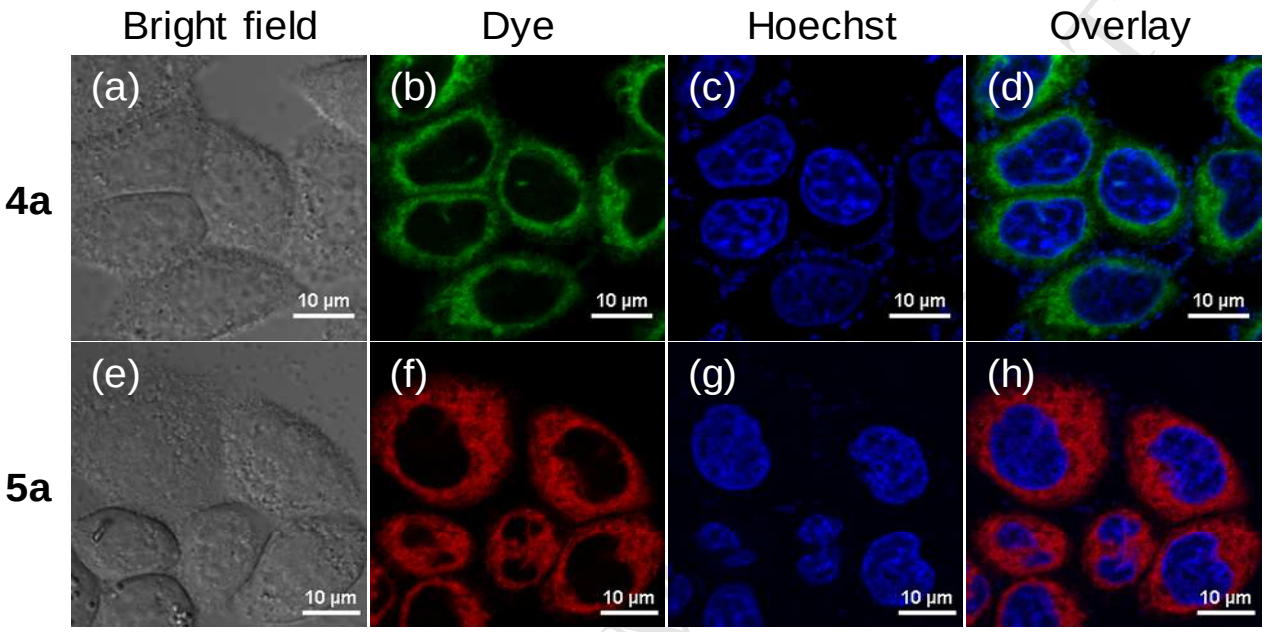

Fig. 8 Confocal fluorescence images of HeLa cells stained with Hoechst (1 μM) and dye **4a**/**5a** (10 μM). (a, e) Bright field image. (b) Image from dye **4a** (green channel: λ_{ex} = 488 nm, λ_{em} = 500–530 nm). (c, g) Image from Hoechst (blue channel: λ_{ex} = 405 nm, λ_{em} = 425–475 nm). (d) Merged image of (b) and (c). (f) Image from dye **5a** (red channel: λ_{ex} = 543 nm, λ_{em} = 560–610 nm). (h) Merged image of (f) and (g). Scale bar: 10 μm.

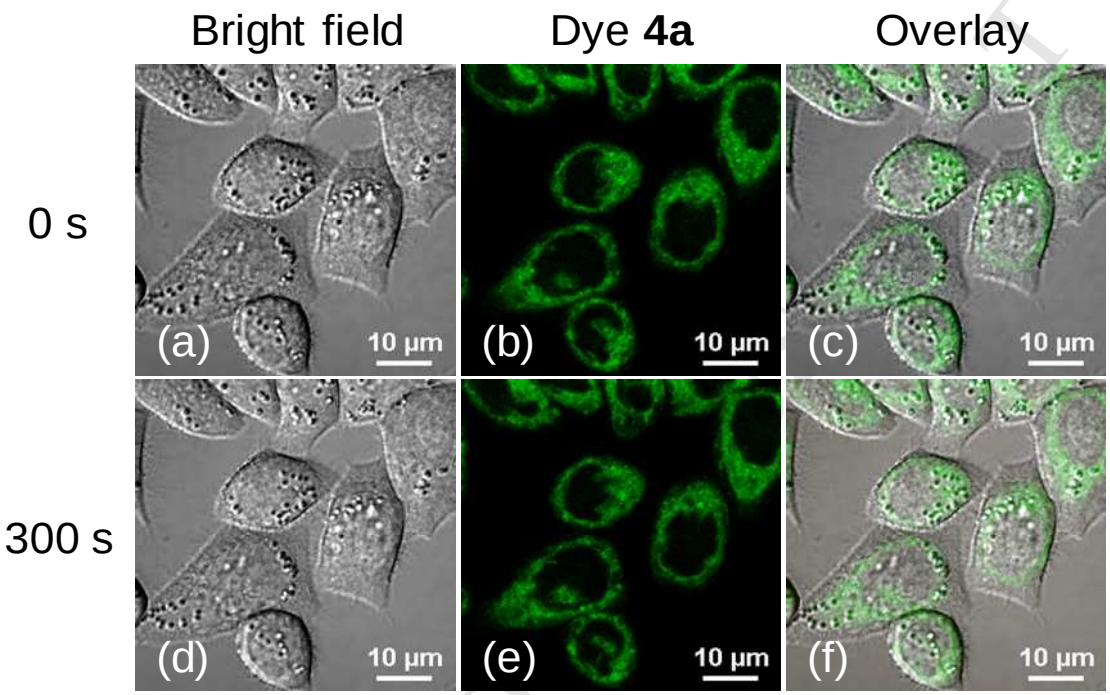

Fig. 9 Confocal fluorescence images of HeLa cells stained with dye **4a (10** μM) at different time points. (a, d) Bright field image. (b, e) Image from dye **4a** (green channel: λ_{ex} = 488 nm, λ_{em} = 500–530 nm). (c) Merged image of (a) and (b). (f) Merged image of (d) and (e). Scale bar: 10 μm.

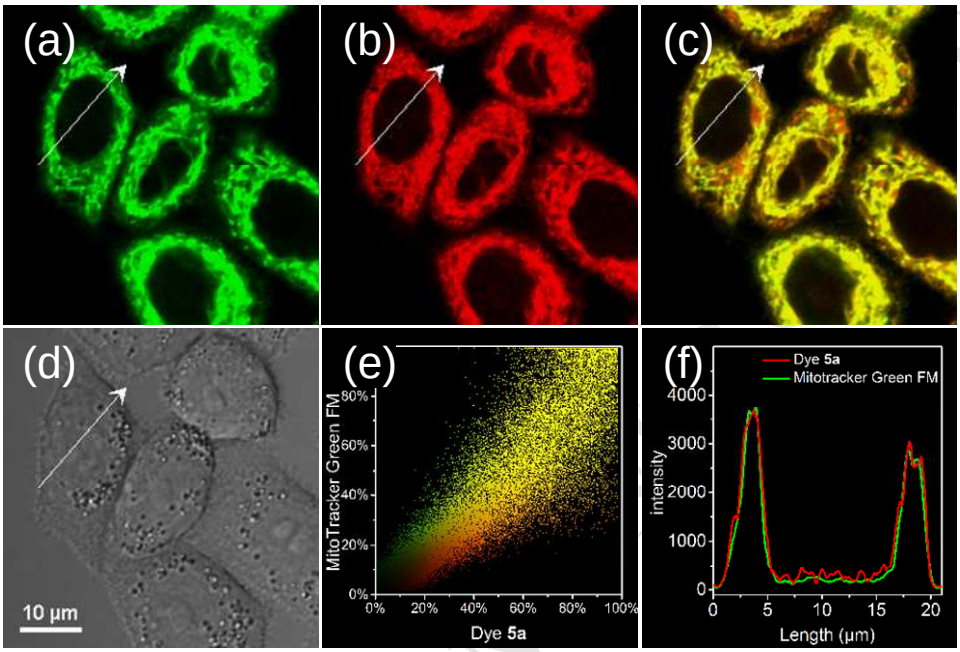

Fig. 10 Confocal fluorescence images of HeLa cells stained with (a) 200 nM MitoTracker Green FM (green channel: λ_{ex} = 488 nm, λ_{em} = 500–530 nm) and (b) 10 μM dye **5a** (red channel: λ_{ex} = 543 nm, λ_{em} = 560–610 nm). (c) Merged image of (a) and (b). (d) Bright field image. (e) Correlation plot of MitoTracker Green FM and dye **5a** intensities. (f) Intensity profile of regions of interest (ROI) across HeLa cells. Scale bar: 10 μm.

Highlights

- A family of anthracene carboxyimides with multi-color fluorescence have been successfully prepared.
- The steady-state, time-resolved and solvatechromic fluorescence of the anthracence carboxyimides could be modulated by changing the substitution groups.
- The anthracene carboxyimides shows high photostability and good cell staining properties.
- Red fluorescent **5a** shows a specific mitochondria-targeting effect.